Measurements of macro- and microscale mixing by Two-Color Laser Induced Fluorescence

K. Kling, D. Mewes,
Institute of Process Engineering, University of Hannover,
Callinstr. 36, 30167 Hannover, Germany
e-mail: dms@ifv.uni-hannover.de

Abstract

Two-Color Laser Induced Fluorescence (LIF) Technique enables the measurement of the progress in mixing on macro- and microscale simultaneously. This is done by injecting a mixture of an inert and a reacting fluorescent dye into the vessel. The inert dye serves as a tracer for the macromixing but does not predicate the mixing quality on the nano scale. Since the chemical reaction requires mixing on the molecular scale, the reacting dye visualizes the micromixing indirectly. Low Reynolds number measurements are performed in a mixing vessel equipped with a Rushton turbine. Repetitive layers form as the impeller blades create new folds each time they pass by the viewing plane. These lamellar structures can be clearly resolved. Areas of micromixing are detected by calculating the local degree of deviation from the measured concentration fields. They are mainly found in the boundary layer of the lamellas. By choosing a suitable border value for the degree of deviation the lamellas can be classified into a center region which is not micromixed yet, and the boundary layer with a high degree of micromixing. The center and border region is separated by means of mathematical filters and their distance is measured. This is the macroscopic length scale of segregation, which is not influenced by micromixing.

1 Introduction

The homogenization of two multicomponent liquids is often accompanied by a fast chemical reaction. This mixing process is of great technical interest but still is not fully understood. The correlation between the convective transport in the flow field and the diffusive transport as well as the kinetic of the chemical reaction is not predictable yet. For the process of the chemical reaction, complete mixing on the molecular scale is required. Micromixing models exist for turbulent mixing most of which make the assumption that the fluid is completely mixed from a macroscopic point of view. A review of available models is given by Baldyga and Bourne (1999). For the laminar mixing process the composition of the compounds strongly varies with the position in the vessel. Therefore global, averaged values for the mixing quality or the mixing time, are only of restricted importance. The prediction of the local composition on micro scale still is not possible for complex geometries. Ottino (1994) introduced a lamellar model which describes the interplay between stretching, diffusion and reaction at small scales. It can be applied for laminar and turbulent mixing, but the application is limited to simple geometric flow domains. Recently, Muzzio and coworkers (2003, 2002) extended the one-dimensional model to the complex flow in stirred tanks. The stretching of small fluid elements is calculated in a Lagrangian frame of reference. They found that the stretching field in chaotic flow has a controlling influence on reactive processes, when convection, reaction and diffusion occur on the same time scale.

Despite the progress in predicting reactive mixing there is still a need for experiments, visualizing the local distribution of inert and reactive tracers with high spatial and temporal resolution. Laser Induced Fluorescence has proven to be a suitable measurement technique. The visualization of passive scalars show the convective mixing process (Villermaux et al. (1996), Distelhoff and Marquis (2000), Guillard et al. (2000)). In viscous mixing applications stretching and folding occur simultaneously at different rates in each portion of the flow, creating complex, layered (lamellar) structures. Unger and Muzzio (1999) and Lamberto et al. (1996) have shown that chaotic flows are the only effective way to destroy segregation rapidly in these applications. Reactive tracers, mostly pH-sensitive dyes, are used to measure the micromixing indirectly (Bellerose and Rogers (1994), Hong et al. (2002)). The drawback of using just one reactive dye for viscous mixing applications is that zones of micromixing can qualitatively be visualized by detecting the reaction product but the convective transport and the dilution of the dye on the macroscopic scale is unaccounted for: zones without the reaction product can either be not mixed on the molecular scale or not mixed at all. In this article, an experimental technique with high spatial and temporal resolution to determine local measures for the macro- and micromixing in stirred vessels simultaneously is presented.

2 Micro- and Macromixing- the degree of deviation

To separate the transport phenomena for macro- and micromixing, namely convection and diffusion, a mixture of one inert and one reacting dyes is injected into the mixing vessel. The convective transport affects both dyes whereas the micromixing only varies the concentration of the reacting dye since the process of the chemical reaction requires complete mixing on the molecular scale. As a quantitative measure for the progress in micromixing the local degree of deviation

$$\Delta(\vec{x},t) = 1 - \frac{c_{1,react}(\vec{x},t)}{c_1(\vec{x},t)} \tag{1}$$

is defined. It is obtained by comparing the local concentration of the reaction product $c_{1,reac}$ with the concentration c_1 of the reacting dye which would locally appear without the reaction. The latter is calculated from the local concentration of the inert dye c_2 and the initial concentration ratio:

$$c_1(\vec{x},t) = c_2(\vec{x},t)\frac{c_{1,0}}{c_{2,0}} \tag{2}$$

The local degree of deviation equals the conversion rate, that is the portion of the reacting dye which has not reacted yet. For a completely segregated fluid the local degree of deviation is one. During the micromixing it decreases to its minimum value of zero for a completely homogeneous fluid.

3 Fluorescent dyes

The fluorescence intensity emitted by a fluorescent dye I_F is proportional to the intensity of the light absorbed by the dye I, which is calculated by Lambert-Beer's Law. The quantum yield Φ describes the effectiveness of the fluorescent emission:

$$I_F = \Phi I = \Phi I_0 e^{-\varepsilon s c}. \quad (3)$$

I_0 is the intensity of the exciting light, ε is the molar extinction coefficient and s is the length of the measurement volume. For small concentrations eq. (3) can be simplified by a series expansion so that I_F only linearly depends on the concentration c of the dye:

$$I_F = \Phi I_0 K \varepsilon s c \quad (4)$$

K is a parameter depending on the measurement system, considering for example the viewing angle of the detector. For constant parameters $m = \Phi I_0 K \varepsilon s$ only a simple calibration procedure by measuring the fluorescence intensity for known concentrations of the dyes is necessary in order to predict the concentration from measured intensities:

$$I_F = m \cdot c \quad (5)$$

A system of two fluorescent dyes is used for the experiments. The following set of predetermined criteria has to be met: The dyes are required to be excitable at the same wavelength, and their emission characteristics must be distinguishable. Only one of the dyes should undergo a chemical reaction which alters its fluorescent behavior. The kinetics of the chemical reaction must be fast enough for the mass transfer (the mixing) and not the chemical reaction to be the limiting factor. Only in this case the chemical reaction indirectly visualizes the micromixing. Two dyes purchased from Molecular Probes Inc. are used. The fluorescent emission spectra of both dyes are shown in Fig. 1. The reacting dye, fluo-4, is an indicator for Calcium ions which is changing its fluorescent emission characteristics with the formation of a Calcium complex. This is done quasi spontaneously with a time constant of approximately 10^9 l (mol s)$^{-1}$ (Naraghi (1997)). The second dye, carboxy-SNARF, does not react with Calcium ions and therefore serves as the inert dye. On the other hand its absorption and emission spectrum strongly varies with pH so that a constant pH value has to be adjusted. During the experiments a solution of Tris-buffer (Merck KGaA) of pH = 8.2 is used. For that, carboxy-SNARF is excitable at the same wavelength as fluo-4 but can be detected at much longer wavelengths, which allows a separation of the fluorescent light by means of optical filters.

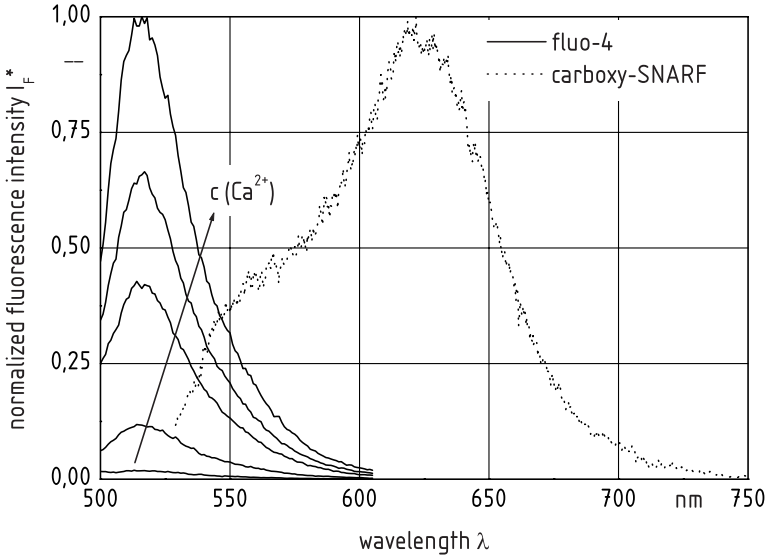

Fig. 1: Normalized fluorescence emission spectrum of fluo-4 and carboxy-SNARF

The reacting dye, fluo-4, is essentially non-fluorescent unless bound to Ca^{2+}. In this case the fluorescence intensity is enhanced depending on the concentration of Calcium ions as shown in Fig. 1. For a concentration of free Ca^{2+} of approx. 40 μmol/l a saturation condition is reached and the fluorescence intensity shows its maximum. Only the saturation condition is used during the experiments since only the concentration of the dye which already reacted with its environment (and therefore is mixed on the molecular scale) is of interest. In order to achieve this a concentration of c(Ca^{2+}) = 0.6 mmol/l is adjusted in the mixing vessel. This high surplus of Calcium ions ensures that the saturation condition is reached immediately in the direct surrounding of the injected dye and the reaction can proceed completely. Highly purified fluo-4 can exhibit a fluorescence enhancement from the minimum value I'_F to the saturation condition I''_F of $\beta = 40 \div 100$ (Haugland, 2002), with

$$\beta = \frac{I''_F}{I'_F}. \tag{6}$$

Due to impurities of Calcium, which are introduced e.g. by the chemicals for the pH- buffer solution or the glassware, there are always free Calcium ions present in the dye solution. This leads to a background fluorescence of fluo-4 and a decreased value of $\beta < 25$. In order to improve the signal-to-noise ratio the background fluorescence must be reduced. For that free Calcium ions, which are introduced due to impurities, are bound to EGTA (SIGMA-ALDRICH Chemie GmbH). EGTA has a higher affinity to Calcium than fluo-4 so that the Calcium ions are no longer available for a reaction with fluo-4. For a concentration of $c_{EGTA} = 7 \cdot 10^{-6}$ mol/l an enhancement factor of β = 58.9 can be measured (Fig. 2).

In Fig. 2 the fluorescence intensities for various concentrations of fluo-4 in a Ca^{2+}-free solution and in saturated condition as well as of carboxy-SNARF is presented. The measured values are approximated with a straight line each according to eq. (5). For both dyes the linear assumption holds only up to a maximum concentration of approximately 10^{-6} mol/l. For higher concentrations quenching effects are not negligible any more so that only dye solutions of lower concentrations should be used. With the calibration factors m_1, m_2 and β, which can be extracted from Fig. 2, the concentrations of the inert dye c_2 and the reaction product $c_{1,reac}$ are calculated from measured fluorescence intensities I_{F1} and I_{F2}:

$$c_2(I_{F1}, I_{F2}) = \frac{I_{F2} - f I_{F1}}{m_2} \tag{7}$$

$$c_{1,reac}(I_{F1}, I_{F2}) = \frac{\beta}{(\beta - 1)} \frac{1}{m_1} \left(I_{F1} - \frac{1}{\beta} \frac{m_1}{m_2} \frac{c_{1,0}}{c_{2,0}} (I_{F2} - f I_{F1}) \right) \tag{8}$$

The parameter $f \approx 0.1$ accounts for the non-ideal behavior of the optical filter for the fluorescence intensity of carboxy-SNARF and has to be determined experimentally. Before the calculation of the concentration fields according to eq. (7) and (8), some corrections are applied. They include the non-uniform illumination of the light sheet due to the intensity profile of the laser beam, the varying intensity of the laser from pulse to pulse and the oblique viewing of the display window from the two apertures of the Double Image Optics (see Chapter “Experimental Set-up”). Details about these corrections can be found in Kling 2003. As a last step the local degree of deviation is calculated according to eqs. (1) and (2).

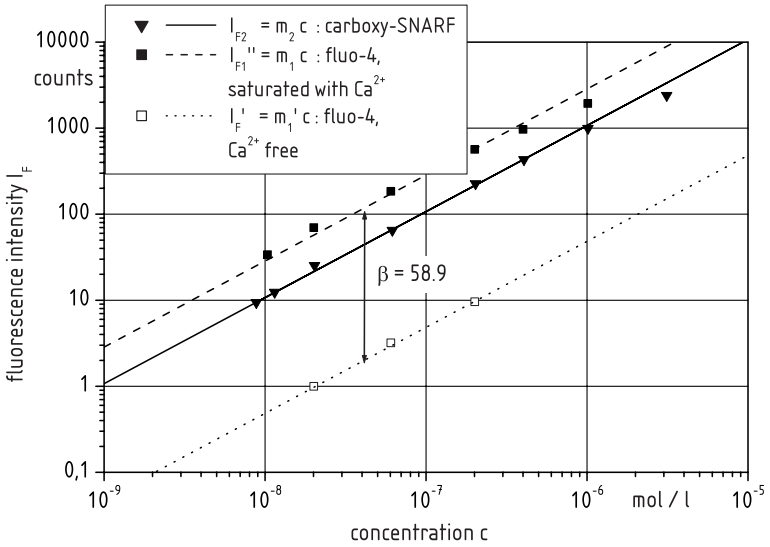

Fig. 2: Fluorescence intensity as a function of dye concentrations

4 Experimental Set-up

The Planar Laser Induced Fluorescence technique (PLIF) is used to measure the concentration fields of two fluorescent dyes simultaneously in the mixing vessel. The optical set-up is schematically depicted in Fig. 3. As a light source a pulsed laser of wavelength λ = 495 nm (NewWave Nd:Yag, Tempest 30 and GWU OPO VisIr) is used. The laser beam is expanded to a thin light sheet using a system of spherical and cylindrical lenses. The divergent light sheet is illuminating an arbitrary plane in the mixing vessel, exciting the fluorescent dye in this area. The emitted light is detected by an intensified CCD-camera (Imager 3 and Image Intensifier, LaVision) which is positioned vertical to the measurement plane. The intensity of the light is measured in 12 bit grey values. The fluorescent light is passing two optical filters (BP523/10 and RG645) which are suitable to separate the fluorescent light of the two dyes. The so-called Double-Image Optics (LaVision) is used to detect the same display window twice at the same time. It consists of two apertures which are equipped with the two filters and a set of adjustable and fixed mirrors. The fluorescent light is reflected by the mirrors onto the light sensitive camera chip such that the same display window is projected side by side on the camera chip with one half each ideally is representing the fluorescent light emitted by one of the fluorescent dyes. The light sheet optics, the mixing vessel and the camera are mounted onto a linear positioning system each in order to allow reproducible adjustments. The exposure of the camera and the pulsation of the laser are controlled by a computer. The maximum measurement frequency is 30Hz and the resolution of the camera is 640 x 480 pixels. With the start of the camera exposure also the injection of the dye is automatically beginning. Each position in the vessel except the position directly underneath the stirrer can be adjusted for the injection. The maximum flow rate amounts 1.25 ml/s but every flow rate below this value can be adjusted.

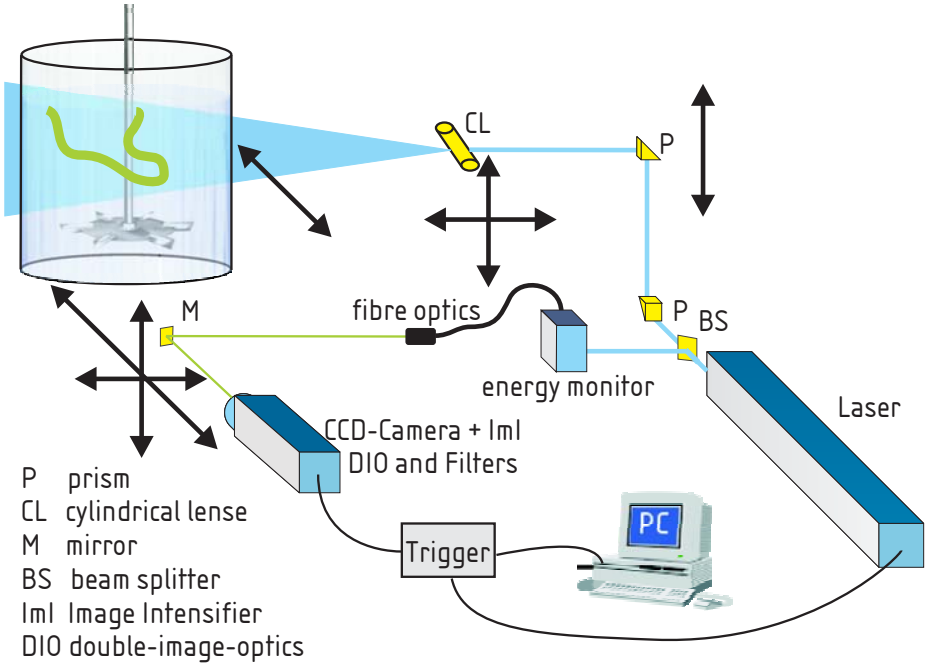

Fig. 3: Optical setup for the Planar Laser Induced Fluorescence (PLIF) Technique

Measurements are performed in a flat-bottomed, transparent vessel of diameter 100 mm. It is placed inside a rectangular viewbox filled with water in order to minimize reflections and distortions at the cylindrical walls. The vessel is filled to a height of 130 mm and the 6-blade Rushton turbine is placed in the vessel with a bottom clearance of 60mm. In order to achieve low Reynolds' number mixing the viscosity of the liquid is increased. This is done by dissolving different mass fractions (0,5%, 1% or 2%) of carboxy-methyl-cellulose (CRT 10000, Wolff Walsrode) in de-ionized water, which leads to a slightly shear thinning behavior of the liquid.

5 Experimental Results

As an example the course of the macro- and micromixing for the cellulose solution with a mass fraction of 1% and the injection position close to the stirrer shaft is shown in Fig. 4. A mixture of the inert dye with $c_{1,0} = 2.2\ 10^{-6}$ mol/l and the reacting dye with $c_{2,0} = 1.02\ 10^{-6}$ mol/l is prepared and a volume of 1 ml is injected into the vessel with a flow rate of 0.5 ml/s after the velocity field had achieved a steady state. The stirrer speed is 300 min^{-1} which leads to a Reynolds number in the laminar region. The display window is situated in the symmetry plane of the vessel whereas the injection position is displaced by an angle of approximately 90°. The display window has a size of 35 mm x 60 mm so that one pixel of the camera chip corresponds to approximately 0.13 mm. The macromixing is represented by the concentration field of the inert dye c_2 and the micromixing is depicted by the field of the local degree of deviation Δ which is calculated from measured dye concentrations.

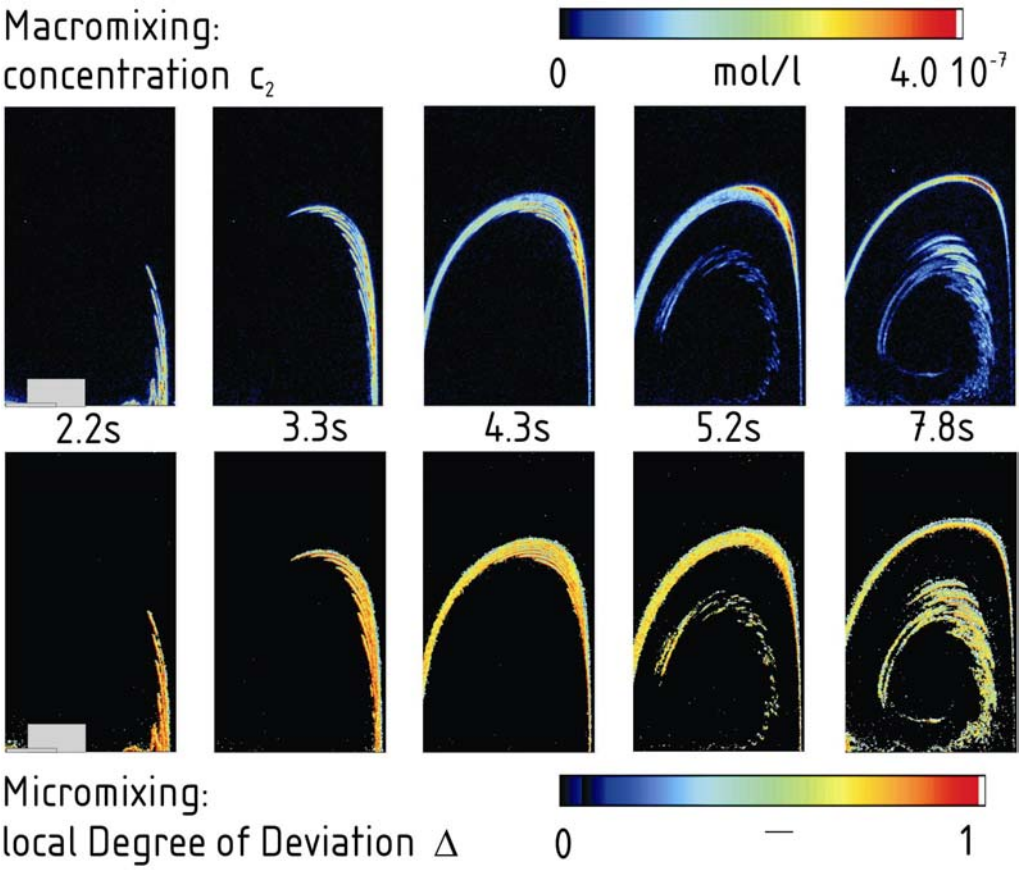

Fig. 4: Course of the macro- and micromixing for the dye injection close to the stirrer shaft

For the injection position close to the stirrer shaft, macro- and micromixing are performed efficiently as presented in Fig. 4. Since the dye is initially injected in a region of high shear rates and high axial velocities it is rapidly transported through the stirrer plane, generating lamellar structures. The repetitive layers which are visible already after 2s form as the impeller blades create new folds each time they pass by the viewing plane. The local degree of deviation is high in the center of the lamellas and already decreased in the boundary layers. The lamellar folds travel towards the wall, deform further, stretch and fold and after 4s recirculate again through the impeller region forming a second loop. After 8s the multi-layered structure can only be resolved in the second inner loop. In the center regions of some lamellas the local degree of deviation is still high, but in large parts it already decreased to a value of approx. 0.4-0.6.

From Fig. 4 it is visible that during the laminar mixing process lamellar structures are formed which consist of repetitive layers with and without the dye. Depending on the viscosity of the fluid and the velocity at the injection position different lamellar structures are forming. The spacing between the layers, the striation thickness, is the macroscopic length scale of segregation. It depends on the position and the residence time in the vessel. For the evaluation of the global mixing quality depending on a change of e.g. geometric or material properties an average value for the striation thickness is calculated. In the following, the determination of the striation thickness is described and the influence of viscosity, rotational speed and injection position is explained in order to verify the method.

From the concentration field it is usually difficult to differentiate between the layers with and without dye because the boundary is not sharp due to diffusive transport. A simple approach is selecting a suitable filter value for the concentration. Hence, fluid elements with $c < c_{filter}$ are assumed to belong to the layer without dye and only fluid elements with $c > c_{filter}$ are assigned to the layer containing the dye. Since during the mixing process the dye is diluted and therefore the concentration strongly varies it is difficult to define a universal filter value. This problem can be overcome by using the field of the local degree of deviation. One example is shown in Fig. 5 and the marked area is enlarged in Fig. 5a. The lamellar structure is clearly resolved. A central region with a high degree of deviation is surrounded by a region with a small degree of deviation. Small values for the local degree of deviation indicate a high progress of micromixing. As expected, micromixing is initiated in the boundary layers.

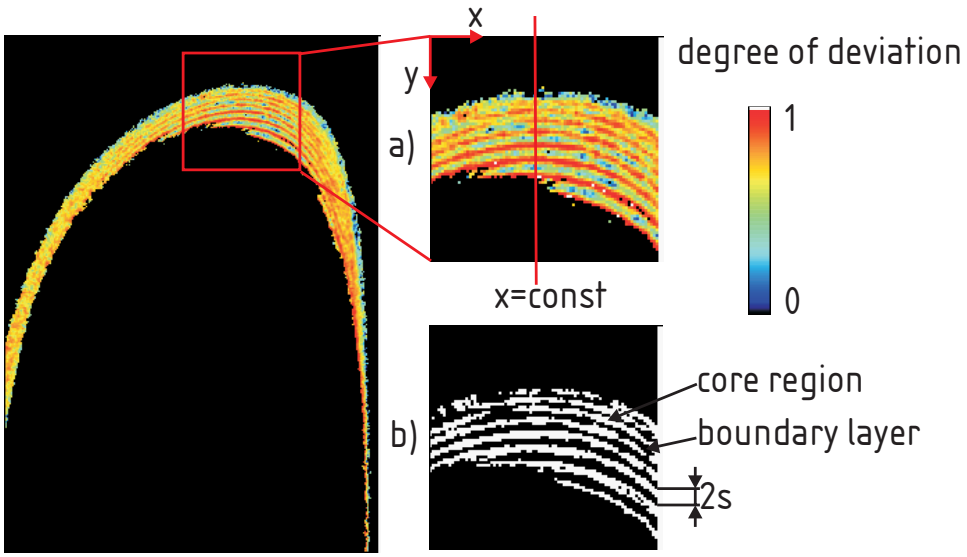

Fig. 5: Field of the local degree of deviation enlarged (a) and binary-coded (b)

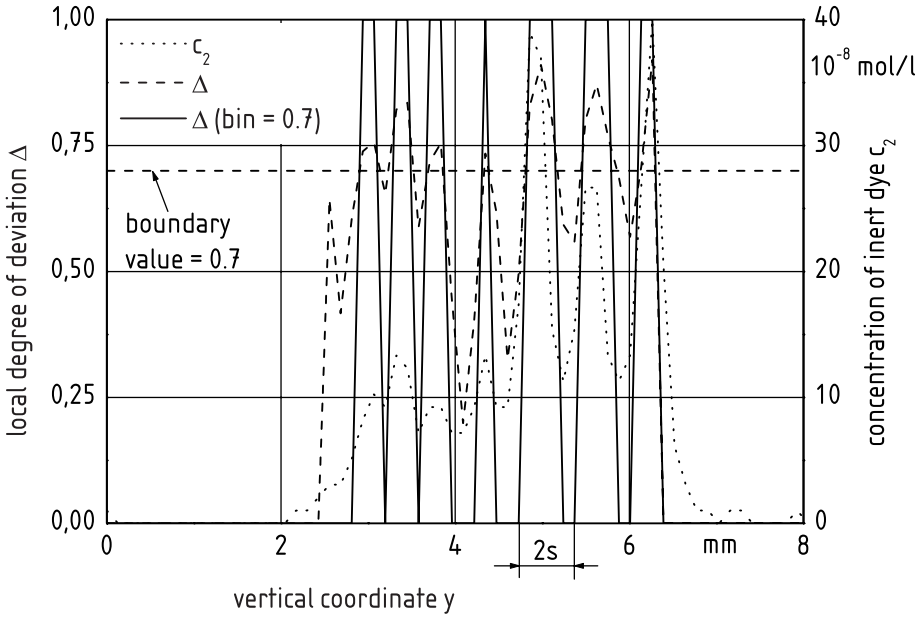

Fig. 6: Profile of the local degree of deviation and the concentration of inert dye

In Fig. 6 the concentration and the degree of deviation is shown along the line of constant x marked in Fig. 5. For distinct peaks of the concentration profile the local degree of deviation takes a value $\Delta > 0.7$. This value is universal and independent of the dilution. Segregated regions can be separated from regions with a high degree of micromixing. Hence, the macroscopic length scale, the striation thickness, can be determined unaffected from the micromixing. For that, the field of the local degree of deviation is binary-coded with the value $\Delta = 0.7$ ($\Delta > 0.7$: $\Delta = 1$; $\Delta < 0.7$: $\Delta = 0$) which is shown in Fig. 5b and results in the compact line in Fig. 6. The striation thickness is half of the distance between two similar layers (with or without dye, respectively).

The striation thickness is determined for various positions and for different times. From that an average value is calculated which is representative for the given settings, eg. viscosity of the liquid, rotational speed and injection position. In Fig. 7 the average striation thickness s_m is presented as a function of the rotational speed with the viscosity and the injection position as parameters. The error bars indicate the standard deviation of the measured results. There are three main conclusions:

1. For the same viscosity of the fluid the striation thickness is decreased with increasing rotational speed.

   For the injection position close to the stirrer shaft (position B) the striation thickness is decreased with increasing rotational speed. The reason is the increased velocity and therefore the faster transport into zones of high shear rates in the impeller region. However, this transport is reduced for the injection position in the center of the vortex (position A). The dye is transported mostly in circumferential direction so that the higher rotational speed does not significantly affect the mixing process and the striation thickness remains nearly constant. For fluids of different viscosity there is no consistent trend for the striation thickness as a function of rotational speed. This is due to the fact that for higher viscous fluids the rotational speed has to be increased in order to receive a similar flow field.

2. With increasing viscosity of the cellulose solution the striation thickness is increased.

   The effect of the viscosity is distinct especially for the two higher viscous fluids. Viscous dissipation causes a diminished secondary flow in the upper and lower vortex compared to the flow in circumferential direction. Therefore the mixing effect due to stretching and folding in the secondary flow is decreased for increasing viscosity. This leads to an increasing striation thickness.

3. The striation thickness depends on the injection position.

   As described above the mixing effect of the secondary flow loop has only a small influence for fluid elements injected in the center of the vortex. Therefore the striation thickness is higher for the injection in the center of the vortex (position A) compared to the injection in regions of high axial velocity close to the stirrer shaft (position B).

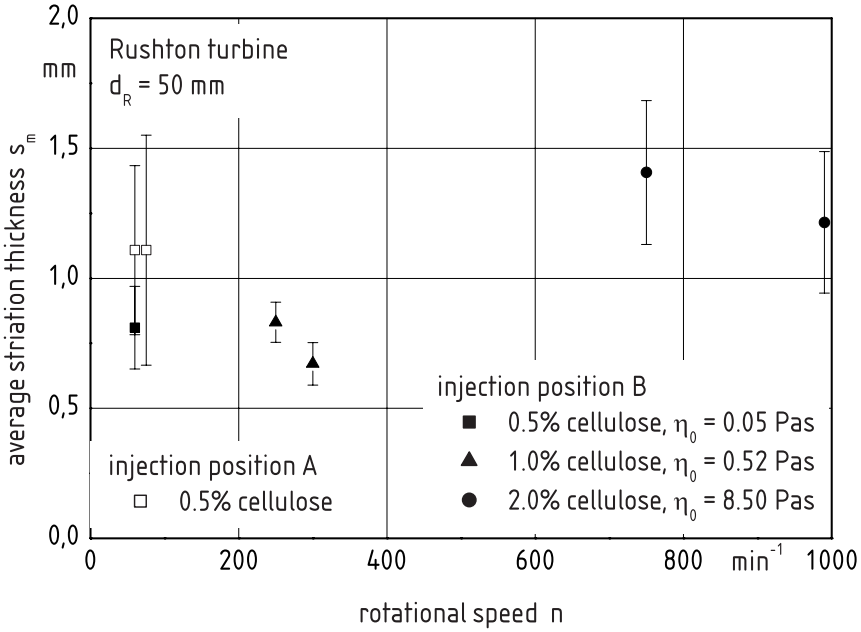

Fig. 7: Average value of the local striation thickness as a function of rotational speed

6 Conclusions

The two-colour Laser Induced Fluorescence Technique gives new insight into the mixing process. It is possible to measure the local intensity of segregation at a multitude of points inside the stirred vessel. This is done by injecting a mixture of an inert and a reacting fluorescent dye into the vessel and by measuring their concentration fields. The fluorescence intensity of the inert dye only depends on its concentration and it therefore serves as a tracer for the macromixing. The fluorescence intensity of the reacting dye instead is enhanced by a chemical reaction which requires mixing on the molecular scale and therefore shows the micromixing. Low Reynolds number measurements are performed in a mixing vessel equipped with a Rushton turbine. The creation of lamellar structures can clearly be resolved. Areas of micromixing are detected by calculating the local degree of deviation from the measured concentration fields. They are mainly found in the boundary layer of the lamellas. By choosing a suitable border value for the degree of deviation the lamellas can be classified into a center region which is not micromixed yet, and the boundary layer with a high degree of micromixing. From that the macroscopic length scale of segregation, the striation thickness, can be determined unaffected by micromixing. The striation thickness is decreased for decreasing viscosity, increasing rotational speed and increasing axial or radial velocity at the injection position.

Acknowledgements

The authors gratefully acknowledge the financial support of the German research Foundation (DFG).

References

Baldyga, J.; Bourne, J.R. (1999): Turbulent mixing and chemical reaction. John Wiley & Sons Ltd.

Bellerose, J.A.; Rogers, C.B. (1994): Measuring mixing and local pH through Laser Induced Fluorescence. Laser Anemometry 191, 217-220.

Distelhoff, M.F.W.; Marquis, A. J. (2000): Scalar mixing in the vicinity of two disk turbines and two pitched blade impellers. Chem. Eng. Sci. 55, 1905-1920

Guillard, F.; Träghard, C.; Fuchs, L. (2000): New image analysis methods for the study of mixing patterns in stirred tanks. Can. J. of Chem. Eng. 78, 273-285.

Haugland, R.P (Edt.) (2002): Molecular Probes- Handbook of Fluorescent Probes and Research Products, 9th Edition.

Hong, S. D.; Sugii, Y.; Okamoto, K.; Madarame, H. (2002): Proceedings of the 10th International Symposium on Flow Visualization, August 26-29, 2002 in Kyoto, Japan, paper F0275.

Kling, K., Mewes, D. (2003): Quantitative Measurements of Micro- and Macromixing in Stirred Vessels using Planar Laser Induced Fluorescence; Journal of Visualization 6, 165-173.

Lamberto D.J., Muzzio F.J., Swanson P.D., Tonkovich A. L. (1996): Using time-dependent RPM to enhance mixing in stirred vessels. Chem. Eng. Sci. 51, 733-741.

Muzzio, F.J.; Alvarez, M.M.; Zalc., J.M.; Shinbrot, T.; (2002): Mechanisms of mixing and creation of structure in laminar stirred tanks. AIChE Journal 48, 2135-2148.

Muzzio, F.J.; Szalai, E.S.; Kukura, J.; Arratia, P.E. (2003): Effect of hydrodynamics on reactive mixing in laminar flows. AIChE Journal 49, 168-179.

Naraghi, M. (1997): T-jump study of calcium binding kinetics of calcium chelators; Cell Calcium 22, 255-268.

Ottino, J.M. (1994): Mixing and chemical reactions - a tutorial. Chem. Eng. Sci. 49, 4005-4027.

Unger, D.R.; Muzzio, F.J. (1999): Laser- Induced Fluorescence technique for the quantification of mixing in impinging jets. AIChE Journal 45, 2477-2486.

Villermaux, J.; Houcine, I.; Vivier, H.; Plasari, E.; David, R. (1996): Planar laser induced fluorescence technique for measurements of concentration fields in continuous stirred tank reactors. Experiments in Fluids 22, 95-102.